Thermally Induced Hydrodynamic Fluctuations below the Onset of Electroconvection

I. Rehberg, S. Rasenat, M. de la Torre Juárez, W. Schöpf, F. Hörner, G. Ahlers,[a] and H. R. Brand[b]
Physikalisches Institut, Universität Bayreuth, W-8580 Bayreuth, Germany
(Received 4 December 1990).

Measurements of the correlation function below the electrohydrodynamic instability in a thin layer of a nematic liquid crystal reveal fluctuating convection patches. Their amplitude $\bar{A}$, correlation length ξ, and correlation time τ can be described by a stochastic mean-field model. The amplitude agrees with the expected fluctuations due to thermal noise.

PACS numbers: 47.20.−k, 05.40.+j, 61.30.Gd

In thermodynamic systems near critical points, thermal noise leads to fluctuations in the order parameter with characteristic size ξ and lifetime τ, which diverge at the critical temperature T_c [1]. For the case of the liquid-gas or liquid-mixture critical point, where the order parameter is directly coupled to the density, the fluctuations become visible close to T_c (critical opalescence) [1]. Large fluctuations lead to critical behavior which differs from that predicted by mean-field theory [1]. Analogous phenomena are expected to occur also in nonequilibrium systems [2]. However, so far fluctuations have been observed only near the threshold of a laser [3], where there are no spatial variations [4]. In that case, the experimental results can be explained [5] in terms of a single-mode stochastic model. Examples involving *spatial* degrees of freedom are hydrodynamic instabilities [2,6–8]. However, for those systems fluctuations were regarded as unobservably small because of their macroscopic character leading to characteristic dissipative energies many orders of magnitude larger than k_BT [9]. Nonetheless, by choosing a particularly favorable hydrodynamic system and using digital enhancement of the signal-to-noise ratio [10] we have been able to measure quantitatively the amplitude $\bar{A}$, spatial extent ξ, and lifetime τ of the fluctuations. The results agree with a stochastic model for a spatially extended system with a noise intensity corresponding to the thermal energy k_BT, but cannot be explained by a single-mode model.

The measurements became possible by investigating electroconvection (EC) [11] in a thin layer of a nematic liquid crystal. Here fluctuation effects are relatively large because the transport coefficient which determines the dissipative energy is small [2], and because a layer of rather small thickness d can be used. The total gain in the effective noise intensity compared to Rayleigh-Bénard convection (RBC) in water is typically 4 orders of magnitude.

We used a layer of thickness $d=13\pm2$ μm of the nematic liquid crystal *N*-(*p*-methoxybenzylidene)-*p*-butylaniline (MBBA). A preferred direction of the rolls above onset is enforced by rubbing the glass slides which confine the sample. The temperature is controlled to ±0.01 K. The rms value V of the ac voltage (45 Hz) is the control parameter, and can be changed in steps of 0.0035 V. The shadowgraph intensity $I(x,t)$ is digitized at various times t and at 512 positions x along a line parallel to the wave vector of the convection rolls over a length of $13.4d$ (the entire sample is about 100 times longer than this). The modulation of the light intensity is proportional to the director angle θ, which allows the measurement of $\bar{A}=\langle\theta^2\rangle^{0.5}$ as described elsewhere [10,12].

In the bottom part of Fig. 1 we show $\bar{A}$ as a function of the applied voltage. The squares are for increasing and the circles for decreasing voltage. Unexpectedly, the bifurcation is hysteretic. The fully developed nonlinear convection rolls above the jump are stationary. Because of the hysteresis and the fluctuations, the last point measured below the transition at $V=7.134$ V is only a lower bound for the subcritical instability, which was estimated by a power-law extrapolation of τ to be at $V_c=7.141$ V. This value serves to define the control parameter $\varepsilon=(V/V_c)^2-1$. The finite value of $\bar{A}$ on the lower branch of the hysteresis loop stems from fluctuating convection rolls. As indicated in the top part of Fig. 1, the wave number k of these fluctuations smoothly joins those

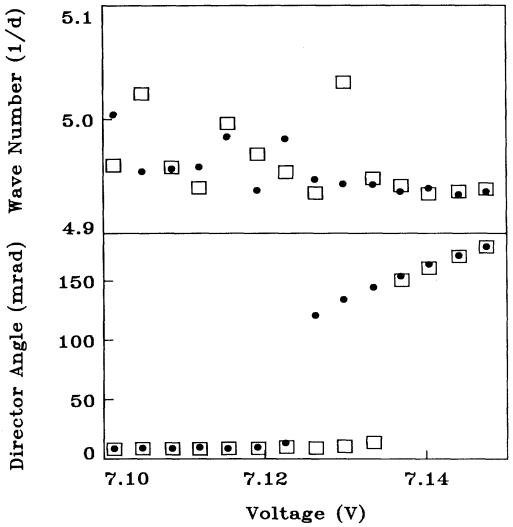

FIG. 1. $\bar{A}$ and k measured at increasing (□) and decreasing (●) ε.

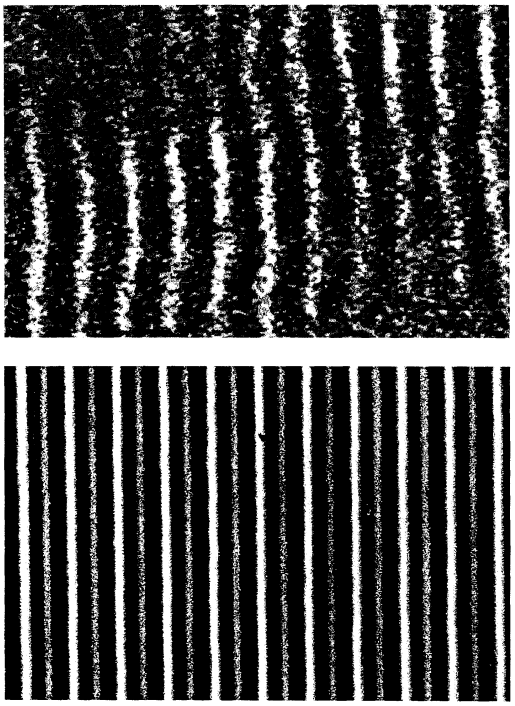

FIG. 2. Spatial structure of the fluctuations below V_c (top), and of fully developed convection (bottom), in a rectangle of $13.4d \times 9.3d$. The contrast in the top part is enhanced by a factor of 5.

of the fully convecting state.

An image of the fluctuations at $\varepsilon = -0.003$ is shown in the top part of Fig. 2 (for comparison, fully developed convection rolls at $\varepsilon = 0.001$ are shown in the bottom part of Fig. 2). It is apparent that both the amplitude and the orientation of the rolls deviate from uniformity and participate in the fluctuations. Their temporal behavior is shown in Fig. 3. Successive measurements along one line perpendicular to the rolls are displaced downwards in the vertical direction. Clearly, permanent rolls do not exist, but fluctuating regions of characteristic spatial and temporal extent consisting of rolls with a wavelength similar to that of fully developed convection are visible. The rolls drift irregularly to the right or left. Their temporal correlation (see below) suggests that they are the superposition of right- and left-traveling waves of independent and randomly varying amplitudes.

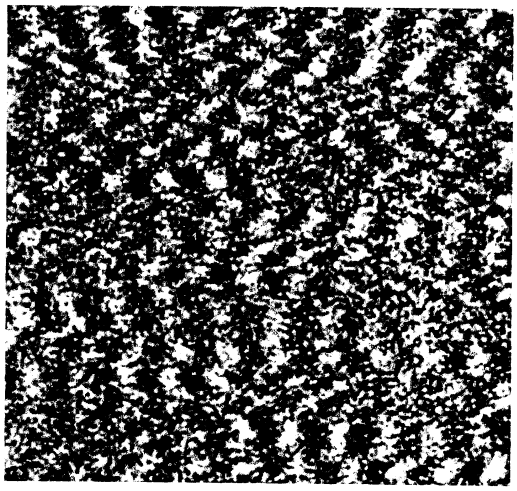

FIG. 3. Temporal development of a line of length $13.4d$ measured over a time of 512 s.

We measured the correlation function $C(\Delta x, \Delta t) = \langle I(x,t) I(x+\Delta x, t+\Delta t) \rangle$ of the fluctuations at a given ε. Figure 4 shows an example of $C(\Delta x, \Delta t)$ for several discrete values Δt at $\varepsilon = -0.007$. The data for $C(\Delta x, 0)$ are not shown because they are perturbed by instrumental noise [10]. The correlation function vanishes for $\Delta t = 5.6$ s and then increases again. This is indicative of the superposition of right- and left-traveling waves in statistically equal proportions. The spatial and temporal decays and the well-defined wavelength of the fluctuations are apparent.

A theoretical expression for the correlation function is derived from a linearized envelope equation representing, e.g., a left-traveling wave in an anisotropic system:

$$\tau_0(\partial_t + s\,\partial_x)A = \varepsilon A + \xi_{\parallel}^2 \partial_{xx}^2 A + \xi_{\perp}^2 \partial_{yy}^2 A + \sqrt{Q} F(x,y,t)\,, \tag{1}$$

where $\sqrt{Q}F(x,y,t)$ models the noise with its spatiotemporal correlation given by

$$\langle F^*(x,y,t) F(x+\Delta x, y+\Delta y, t+\Delta t) \rangle = \delta(\Delta x)\delta(\Delta y)\delta(\Delta t)\,.$$

For simplicity all coefficients in Eq. (1) are taken real. In a first approach we neglect the y dependence. One obtains for the envelope of the space-time correlation in this one-dimensional problem the analytic result

$$C_l(\Delta x, \Delta t) \equiv \langle A^*(x,t) A(x+\Delta x, t+\Delta t) \rangle = \bar{A}^2 \left\{ \exp\left[-\left(\frac{\Delta x}{\xi} - \frac{\Delta t}{\sigma} \right) \right] \operatorname{erfc}\left\{ \left(\frac{\Delta t}{\tau} \right)^{1/2} - \frac{1}{2} \left[\frac{\Delta x/\xi}{(\Delta t/\tau)^{1/2}} - \left(\frac{\Delta t \tau}{\sigma^2} \right)^{1/2} \right] \right\} + \exp\left[+\left(\frac{\Delta x}{\xi} - \frac{\Delta t}{\sigma} \right) \right] \operatorname{erfc}\left\{ \left(\frac{\Delta t}{\tau} \right)^{1/2} + \frac{1}{2} \left[\frac{\Delta x/\xi}{(\Delta t/\tau)^{1/2}} - \left(\frac{\Delta t \tau}{\sigma^2} \right)^{1/2} \right] \right\} \right\}, \tag{2}$$

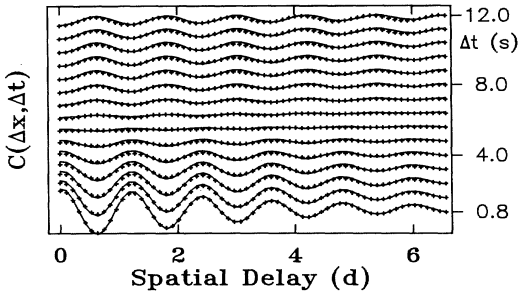

FIG. 4. Spatiotemporal correlation function measured at $\varepsilon=-0.007$. The solid line is a fit of the function $C_{\rm env}\times\cos(kx)\cos(\omega t)$.

with

$$\bar{A}^2=Q/8\tau_0\xi_\parallel(-\varepsilon)^{1/2}. \quad (3)$$

The two correlation times $\tau=\tau_0/(-\varepsilon)$ and $\sigma=\xi_\parallel/s(-\varepsilon)^{1/2}$ measure the (nonexponential) decay of a spatially uniform and a spatially modulated state, respectively, and $\xi=\xi_\parallel/(-\varepsilon)^{1/2}$ is the correlation length. The correlation C_r due to the right-traveling wave is similar, with s replaced by $-s$, and the measured correlation is the sum $C_{\rm env}=C_l+C_r$. We fit $C=C_{\rm env}\cos(kx)\cos(\omega t)$ to the measured correlation functions by adjusting Q, ξ, τ, s, k, and ω. The solid lines in Fig. 4 represent such a fit. In Fig. 5 we show ξ and τ obtained from these fits as a function of ε. The solid lines are fits by $\tau=\tau_0/(-\varepsilon)$ and $\xi=\xi_\parallel/(-\varepsilon)^{1/2}$ and yield $\xi_\parallel=(0.32\pm0.03)d$ and $\tau_0=0.074\pm0.001$ s. The value of $\xi_\parallel$ agrees with the one for a stationary bifurcation fairly well, while τ_0 is about a factor of 2 larger than in the stationary case [13]. The fluctuation amplitudes $\bar{A}$ for $\varepsilon<0$ are shown in Fig. 6. The solid line is a fit of Eq. (3) to the data. Using the measured value for $\tau_0\xi_\parallel$, one gets $Q=2.6\times10^{-7}$.

A calculation of $\bar{A}$ from the two-dimensional model (1) leads to divergences for large wave numbers. They can be traced back to the fact that in the derivation of the envelope equation only slow spatial variations on the scale of the roll wavelength are considered. To avoid the divergences within this model two wave-number cutoffs are introduced as fit parameters. The short-dashed line in Fig. 6 represents such a fit [14]. For comparison, the prediction for $\bar{A}$ based on a single-mode model $\tau_0\dot{A}=\varepsilon A+\sqrt{Q}F(t)$, with $\langle F(t)F(t+\Delta t)\rangle=\delta(\Delta t)$, is shown as well (long-dashed line). This curve, $\bar{A}\sim(-\varepsilon)^{-1/2}$, does not fit the data—an explanation of the experimental results is possible only when spatial degrees of freedom are included. The fact that the one-dimensional model gives a quite good fit to the data already deserves further investigation.

To compare the noise intensities predicted from irreversible thermodynamics with those found experimentally, we follow Ref. [2], p. 269. Considering the dynamic equation for the director $\partial_t(\partial_x n_3)+(\partial_x n_3)=F_3$ ($n_3\approx\theta$, F_3 is the strength of the noise) and neglecting dissipative cross couplings (e.g., to the electric field) which arise as higher-order gradient terms [15], one gets for the correlation function

$$\langle F_3(x,t)F_3(x+\Delta x,t+\Delta t)\rangle=2Q_2\delta(\Delta x)\delta(\Delta t),$$

with $Q_2=k_BT/\bar{K}d$. For the director fluctuations with wave number k_c this yields $\langle\theta^2\rangle=Q_2/k_c^2$. (Times are scaled with $\rho\gamma_1/\bar{K}k_c^2$, ρ is the density, γ_1 is the relaxation constant of the director, and $\bar{K}$ measures the elastic energy.) Inserting the rescaled noise strength into Eq. (1) leads to $Q=(1.8\pm0.3)\times10^{-7}$. This predicted value agrees with the measured value of $(2.6\pm0.3)\times10^{-7}$ fairly well, thus indicating that the fluctuations are due to thermal noise. However, a more quantitative theoretical estimate of the thermally induced fluctuation amplitude would be desirable.

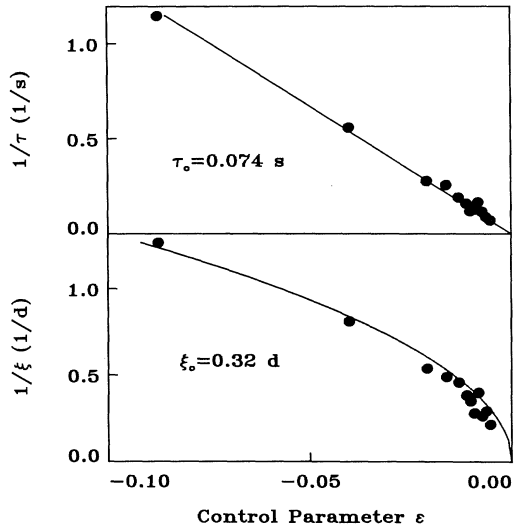

FIG. 5. The inverse of ξ and τ measured as a function of ε. The lines are fits according to the expected power laws.

While the standard deterministic models for EC yield a *forward stationary* bifurcation [16], we find at our driv-

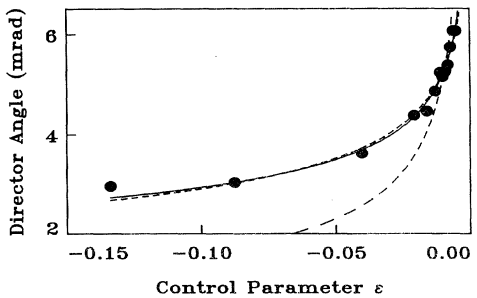

FIG. 6. $\bar{A}$ measured at subcritical values of ε. The lines are fits according to the single-mode (long-dashed), one-dimensional (solid), and two-dimensional (short-dashed) theories.

ing frequency and for our sample thickness a *backward oscillatory* bifurcation. It was found experimentally that thin samples, pure crystals, and high voltages favor an oscillatory bifurcation [17]; thus the discrepancy might be due to the simplified modeling of the electric conductance of the nematic [18]. Another possibility for the backward nature is a critical renormalization effect as predicted for RBC [8]. However, EC in nematics is not expected to be in the same universality class as RBC. We are not aware of any predictions applicable to the critical behavior of EC.

The experiments were supported by Deutsche Forschungsgemeinschaft. G.A. acknowledges support through a Senior U.S. Scientist award from the Alexander von Humboldt Foundation, and additional support through Grant No. DOE84 ER13729 from the U.S. Department of Energy. H.R.B. thanks the Deutsche Forschungsgemeinschaft and M.T.J. the Spanish Ministerio de Educatión y Ciencia for support.

[a]Permanent address: Department of Physics and Center for Nonlinear Science, University of California, Santa Barbara, Santa Barbara, CA 93106.

[b]Permanent address: Fachbereich 7, Physik, Universität Essen, W-4300 Essen 1, Germany.

[1] H. E. Stanley, *Introduction to Phase Transitions and Critical Phenomena* (Clarendon, Oxford, 1971).

[2] R. Graham, in *Fluctuations, Instabilities and Phase Transitions,* edited by T. Riste, NATO Advanced Study Institutes, Ser. B, Vol. 11 (Plenum, New York, 1975).

[3] F. T. Arecchi, G. S. Rodari, and A. Sona, Phys. Lett. **25A**, 59 (1967); F. T. Arecchi, M. Giglio, and A. Sona, *ibid.* **25A**, 341 (1967).

[4] We note that in nonlinear optics the experimental study of the influence of spatial variations on pattern formation has just started: F. T. Arecchi, G. Giacomelli, P. L. Ramazza, and S. Residori, Phys. Rev. Lett. **65**, 2531 (1990); J. W. Grantham, H. M. Gibbs, G. Khitrova, J. F. Valley, and Xu Jiajin, Phys. Rev. Lett. **66**, 1422 (1991). There seems to be no experimental study of the interaction of noise and spatial degrees of freedom.

[5] H. Risken and H. D. Vollmer, Z. Phys. **201**, 323 (1967); H. Risken, in *Progress in Optics,* edited by E. Wolf (North-Holland, Amsterdam, 1970), Vol. VIII, p. 239.

[6] V.M. Zaitsev and M. I. Shliomis, Zh. Eksp Teor. Fiz. **59**, 1583 (1970) [Sov. Phys. JETP **32**, 866 (1971)].

[7] R. Graham, Phys. Rev. A **10**, 1762 (1974).

[8] J. Swift and P. C. Hohenberg, Phys. Rev. A **15**, 319 (1977).

[9] The effect of fluctuations has been observed indirectly in thermal convection by C. W. Meyer, G. Ahlers, and D. S. Cannell, Phys. Rev. Lett. **59**, 1577 (1987). However, an explanation of those results in terms of simple stochastic models requires a noise intensity of about $10^4 k_B T$.

[10] The method used to measure small amplitudes is described in detail in I. Rehberg, F. Hörner, and G. Hartung, J. Stat. Phys. (to be published).

[11] See, e.g., P. G. de Gennes, *The Physics of Liquid Crystals* (Clarendon, Oxford, 1973).

[12] S. Rasenat, G. Hartung, B. L. Winkler, and I. Rehberg, Exp. Fluids **7**, 412 (1989).

[13] S. Rasenat, V. Steinberg, and I. Rehberg, Phys. Rev. A **42**, 5998 (1990).

[14] For the two-dimensional model we get

$$\bar{A}^2 = \frac{Q}{2\pi^2 \tau_0 \xi_\perp} \int_0^{k_x^{\mathrm{cut}}} \frac{1}{z} \arctan\left(\frac{k_y^{\mathrm{cut}} \xi_\perp}{z}\right) dk_x ,$$

with $z = (|\varepsilon| + \xi_\parallel^2 k_x^2)^{1/2}$. From the fit in Fig. 6 we obtained $Q = 6.5 \times 10^{-7}$, $k_x^{\mathrm{cut}} = 4.6$, and $k_y^{\mathrm{cut}} = 0.7$, using the measured $\xi_\parallel$ and $\xi_\perp = \xi_\parallel/3$.

[15] H. R. Brand and H. Pleiner, Phys. Rev. A **35**, 3122 (1987).

[16] E. Bodenschatz, W. Zimmermann, and L. Kramer, J. Phys. (Paris) **49**, 1875 (1988).

[17] See, e.g., M. de la Torre Juárez and I. Rehberg, Phys. Rev. A **42**, 2096 (1990), and references therein.

[18] L. Kramer (private communication).

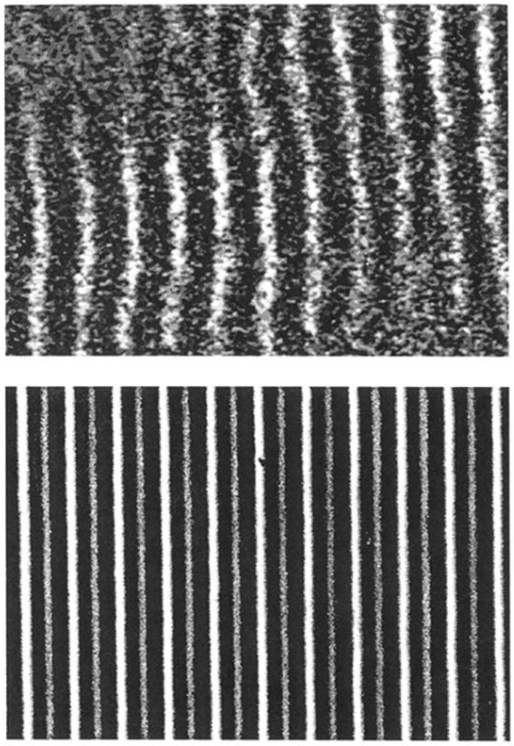

FIG. 2. Spatial structure of the fluctuations below V_c (top), and of fully developed convection (bottom), in a rectangle of $13.4d \times 9.3d$. The contrast in the top part is enhanced by a factor of 5.

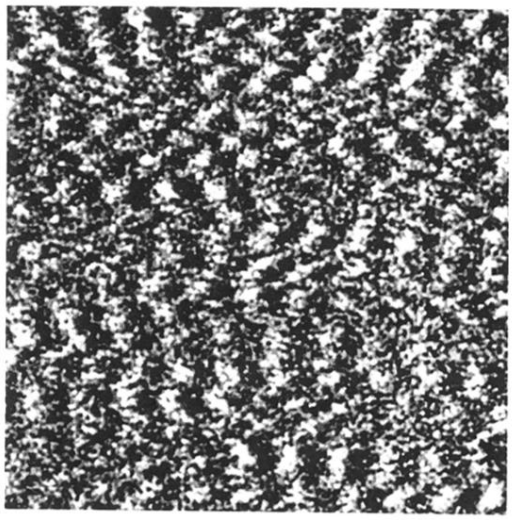

FIG. 3. Temporal development of a line of length 13.4d measured over a time of 512 s.